Supporting Information

Suppression of Homo-Coupling Side Reactions in Direct Arylation Polycondensation for Producing High Performance OPV Materials.

Junpei Kuwabara, Yohei Fujie, Keisuke Maruyama, Takeshi Yasuda, Takaki Kanbara**

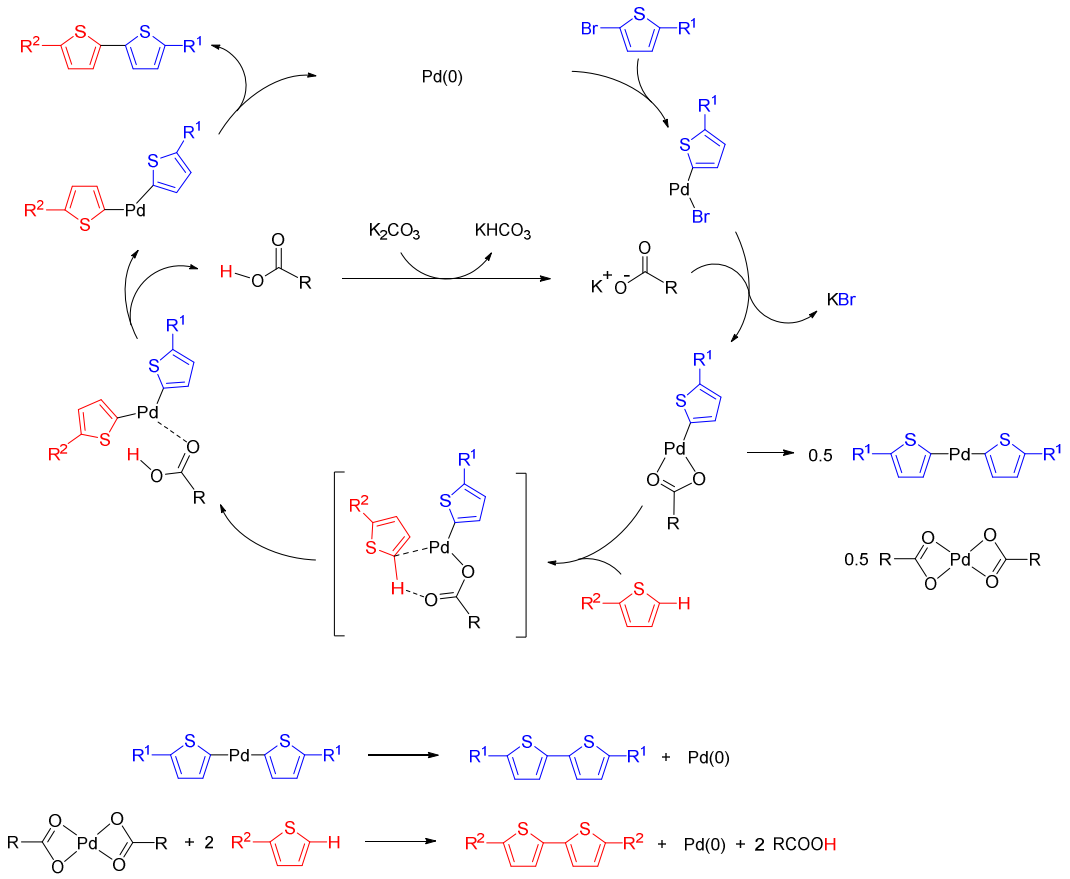

Scheme S1. Proposed mechanism of homo-coupling reaction in direct arylation. A disproportionation reaction of the Pd(II) intermediate forms a biscarboxylato Pd complex and a biaryl Pd complex which affords a C-Br/C-Br homo-coupling compound via reductive elimination. The biscarbocylato Pd complex affords a C-H/C-H homo-coupling compound via C-H bond cleavage.

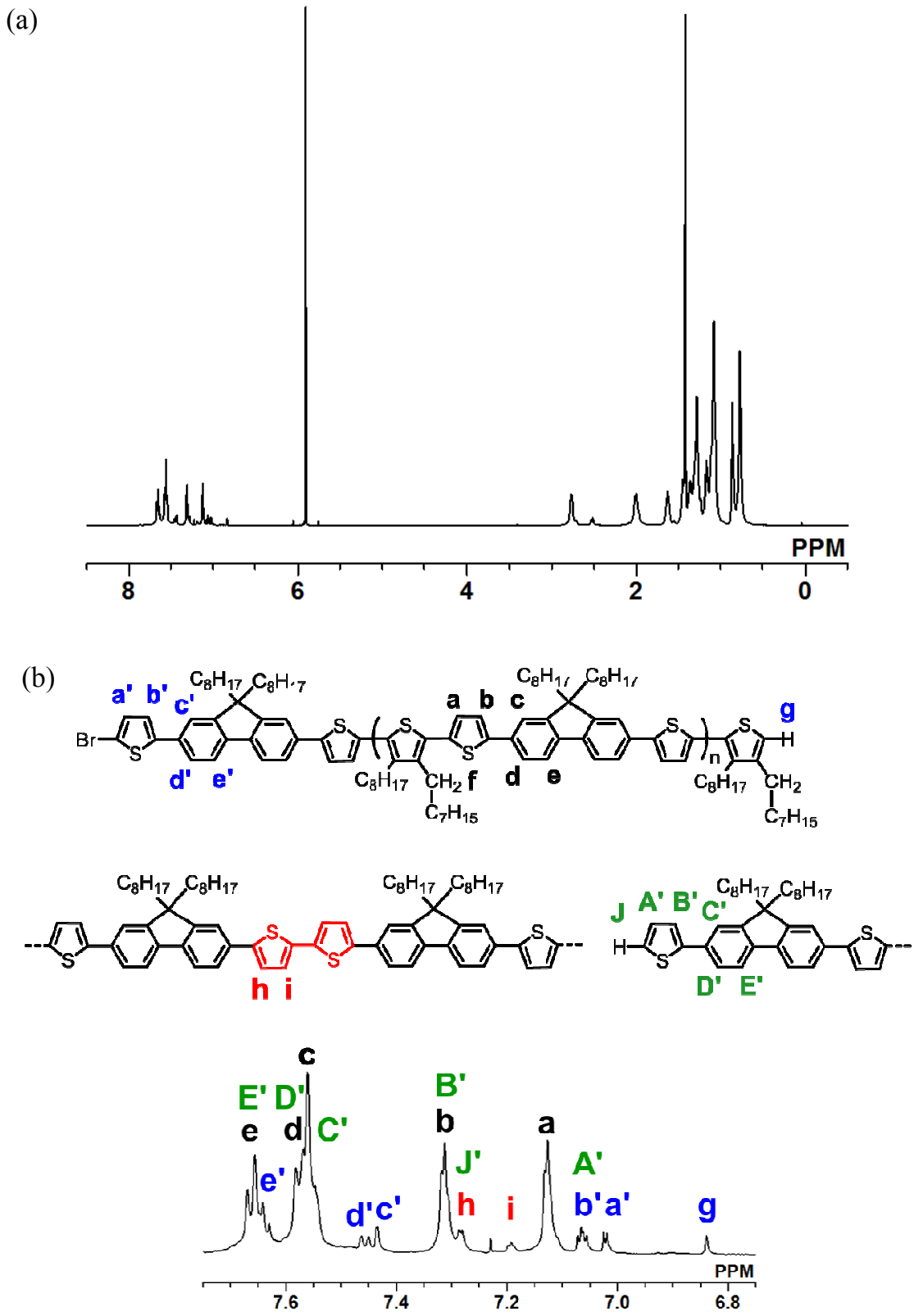

Figure S1. ^{1}H NMR spectrum of **P1** (a) full spectrum (b) aromatic region (600 MHz, $C_2D_2Cl_4$, 353 K). The signl b´ and A´overlap at 7.06 ppm, exhibiting a triplet-like signal.

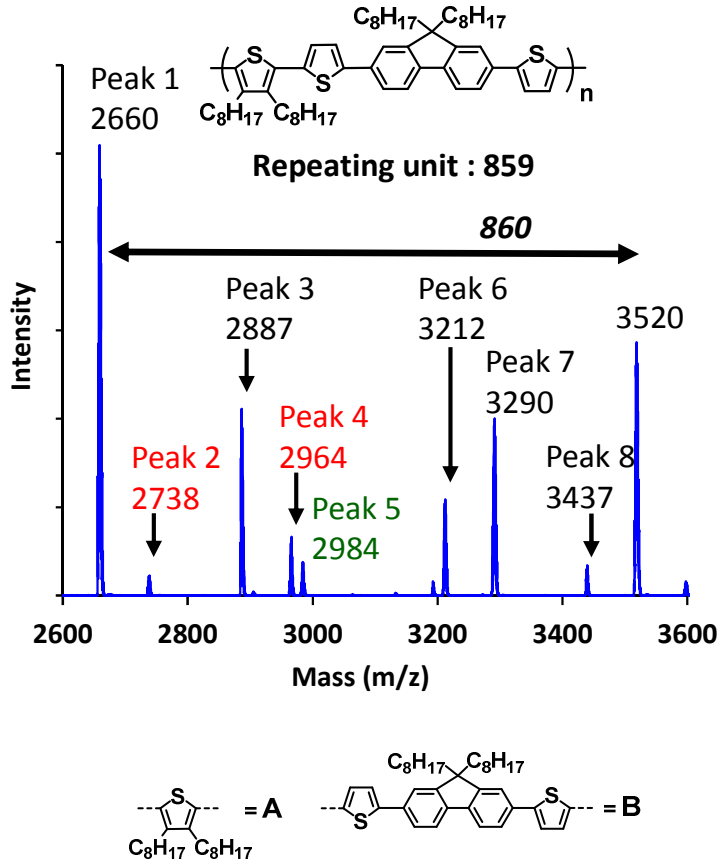

Peak 1 H-(ABABAB)-Br
m/z: 2659

Peak 2 Br-(BAABAB)-Br
m/z: 2737

Peak 3 H-(ABABABA)-H
m/z: 2886

Peak 4 H-(AABABAB)-Br
m/z: 2966

Peak 5 Br-(BABABB)-Br
m/z: 2984

Peak 6 Br-(BABABAB)-Br
m/z: 3212

Peak 7 H-(BABABABA)-H
m/z: 3291

Peak 8 H-(BABABABA)-H
m/z: 3439

Figure S2. MALDI TOF MS spectrum of **P1**.

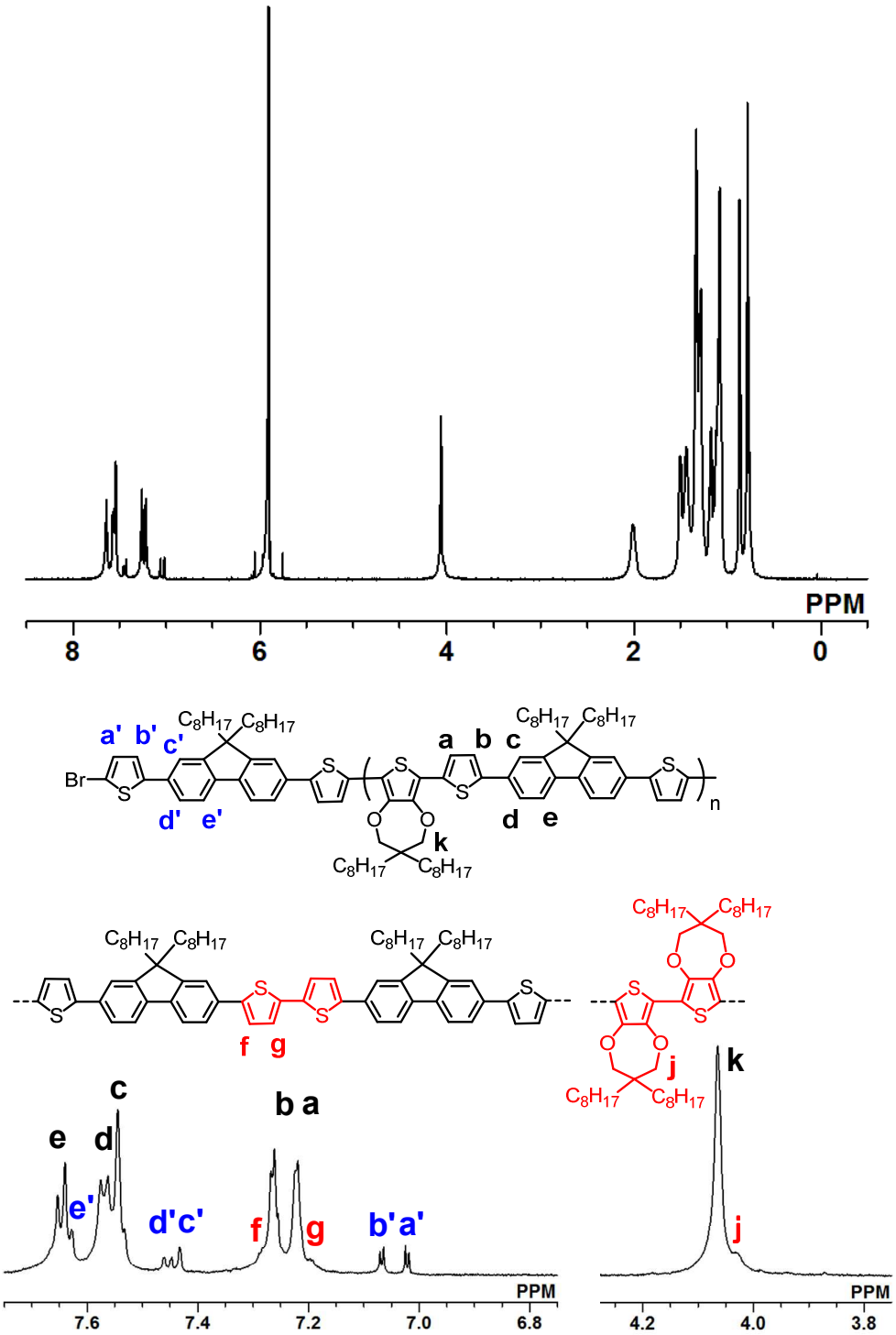

Figure S3. ^{1}H NMR spectrum of **P2** (600 MHz, $C_2D_2Cl_4$, 353 K).

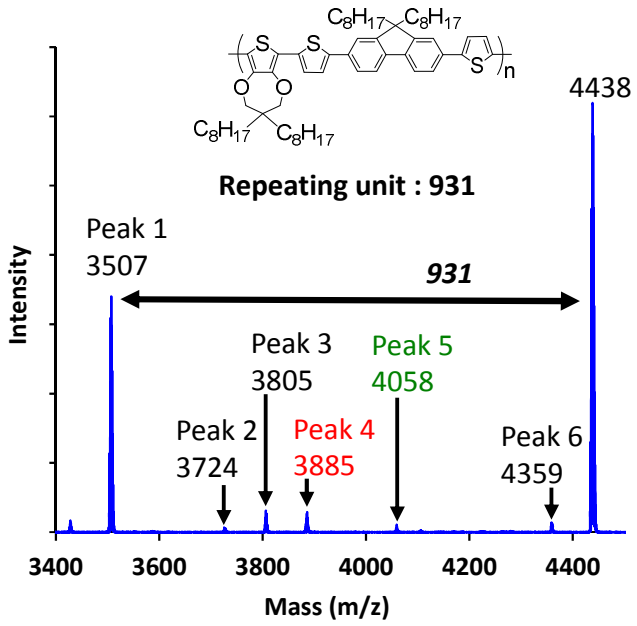

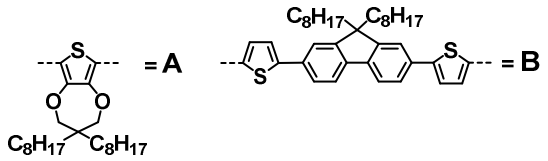

Peak 1 Br-(BABABAB)-Br
m/z: 3507

Peak 2 H-(ABABABAB)-H
m/z: 3727

Peak 3 H-(ABABABAB)-Br
m/z: 3806

Peak 4 Br-(BAABABAB)-Br
m/z: 3885

Peak 5 Br-(BABABBAB)-Br
m/z: 4059

Peak 6 Br-(BABABABAB)-H
m/z: 4359

Peak 7 Br-(BABABABAB)-Br
m/z: 4438

Figure S4. MALDI TOF MS spectrum of **P2**.

(a)

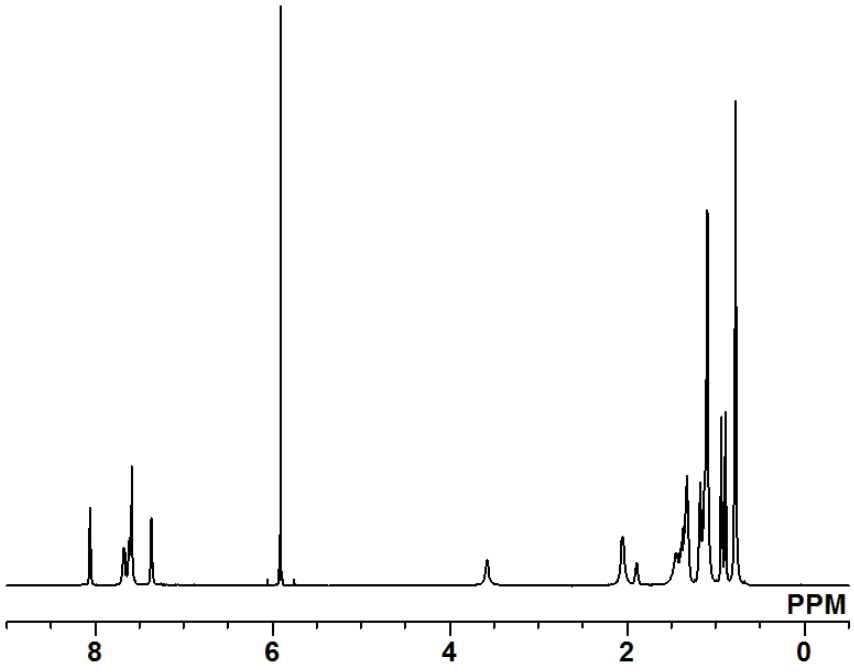

(b)

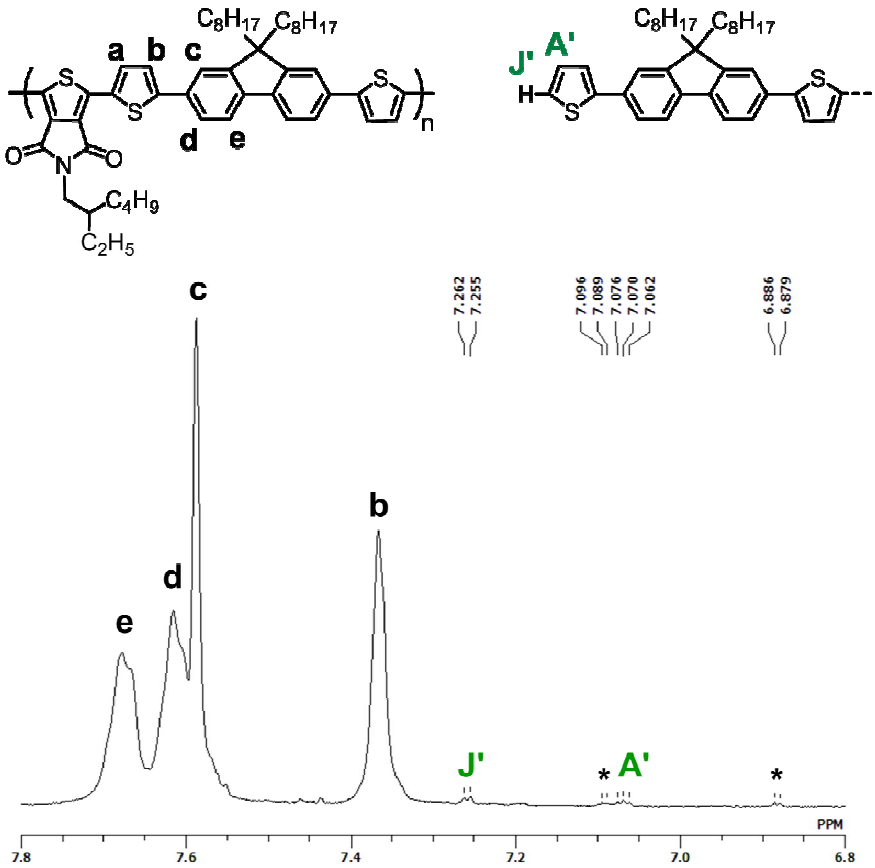

Figure S5. ^{1}H NMR spectrum of **P3** (a) full spectrum (b) aromatic region (600 MHz, $C_2D_2Cl_4$, 353 K). The signals with asterisk could not be assigned.

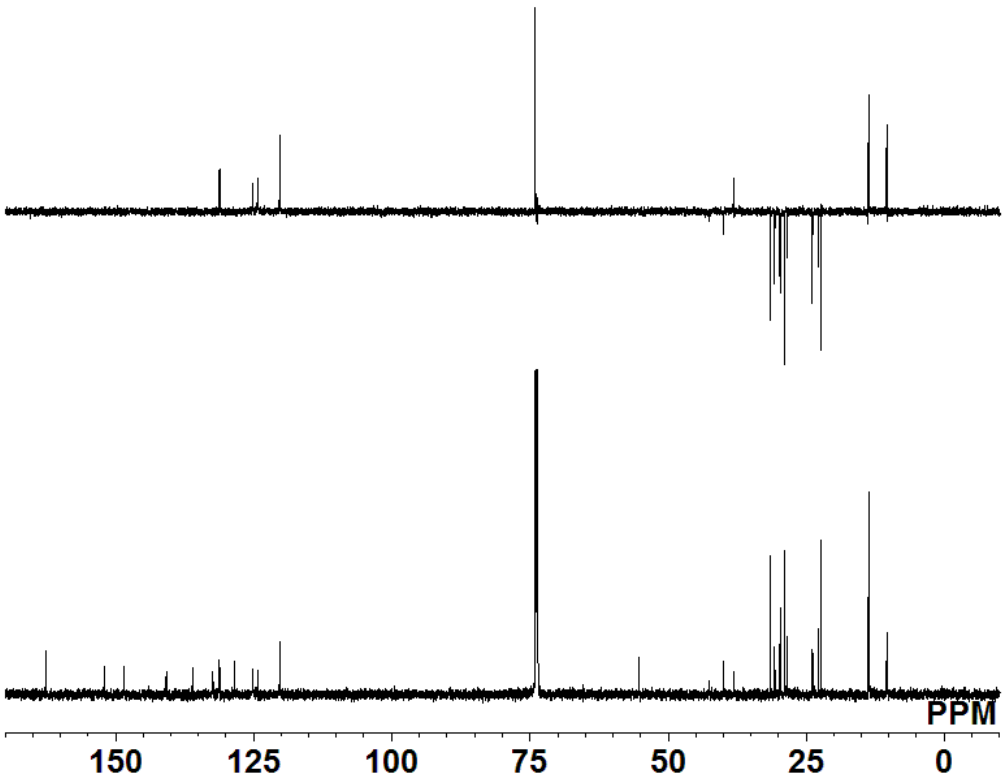

Figure S6. $^{13}C\{^{1}H\}$ and DEPT 135 NMR spectra of **P3** (150 MHz, $C_2D_2Cl_4$, 353 K).

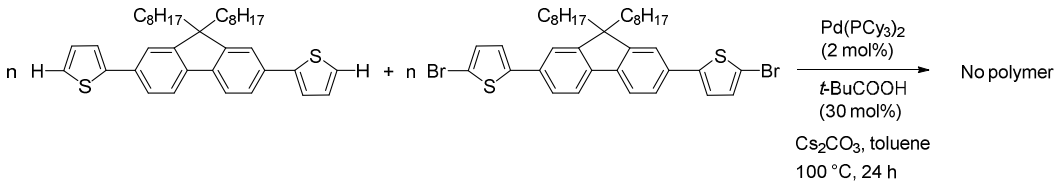

Scheme S2. A control experiment for assessing the reactivity of the C-H bond on the debrominated thienyl group under the toluene system.

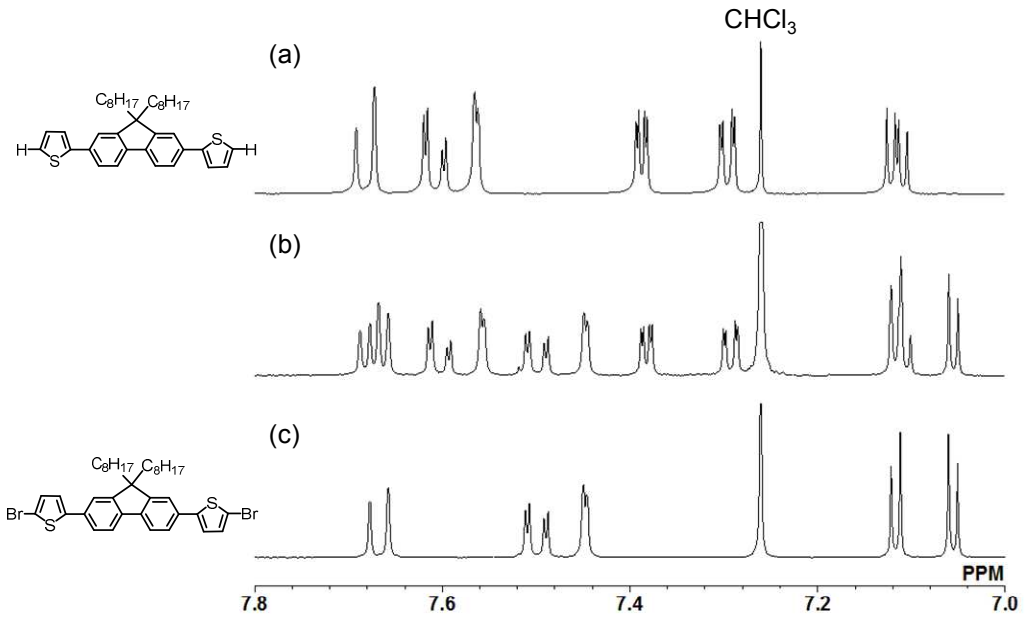

Figure S7. ^{1}H NMR spectra of (a) 2,7-(dithien-2-yl)-9,9-dioctylfluorene, (b) the crude products of the control experiment shown in Scheme S2, and (c) 2,7-bis(5-bromothien-2-yl)-9,9-dioctylfluorene (400 MHz, $CDCl_3$). The spectra reveal almost no reaction of the control experiment shown in Scheme S2, indicating low reactivity of C-H bond on the thienyl group under the toluene system.

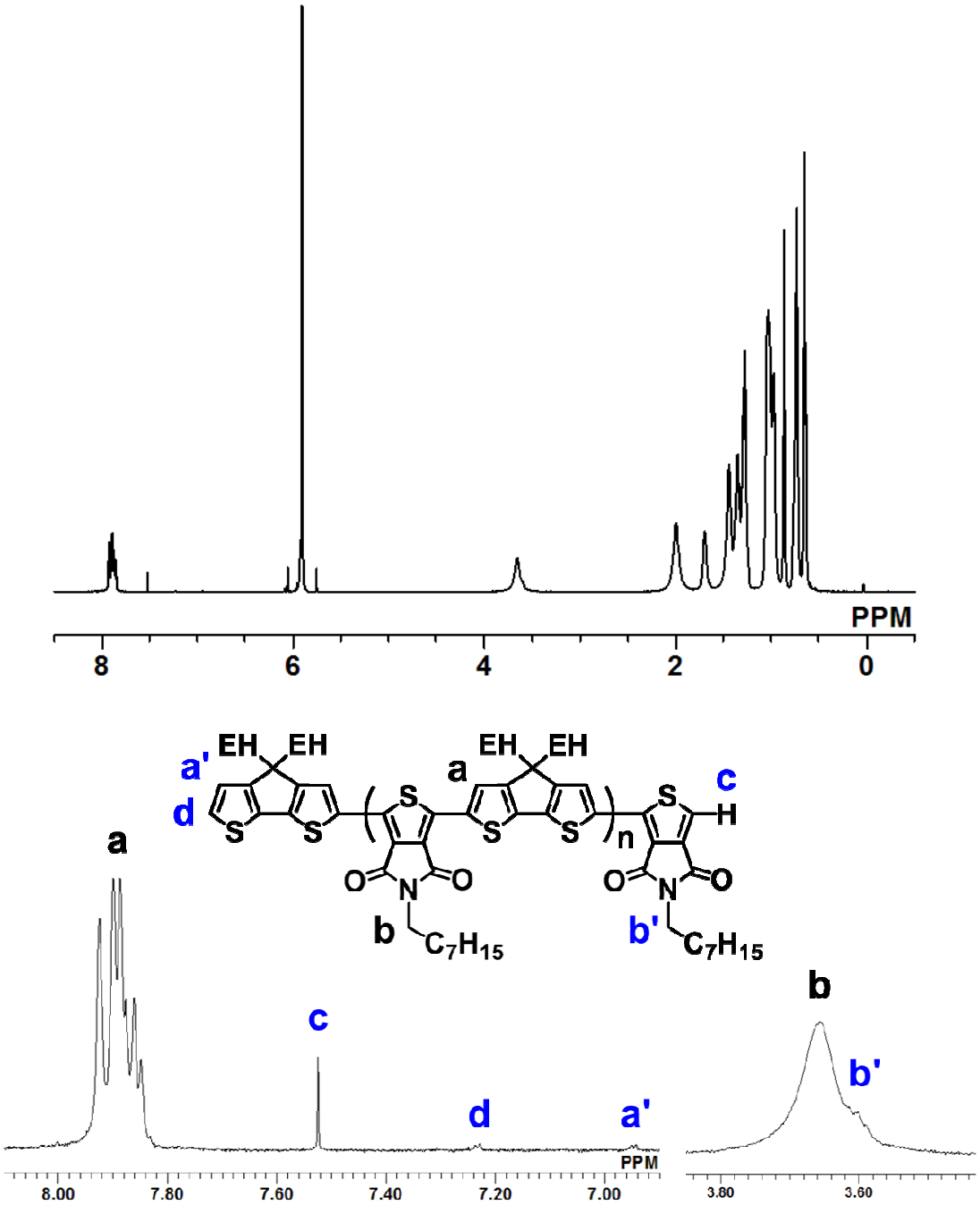

Figure S8. ^{1}H NMR spectrum of **P4** (600 MHz, $C_2D_2Cl_4$, 353 K). Multiplicity of the signal at around 7.89 ppm is due to the presence of diastereomers caused by two 2-ethylhexyl side chain.[S1] No signal for the C-Br/C-Br homo-coupling structures (CPDT-CPDT) was observed at 7.1 and 6.9 ppm.[S1]

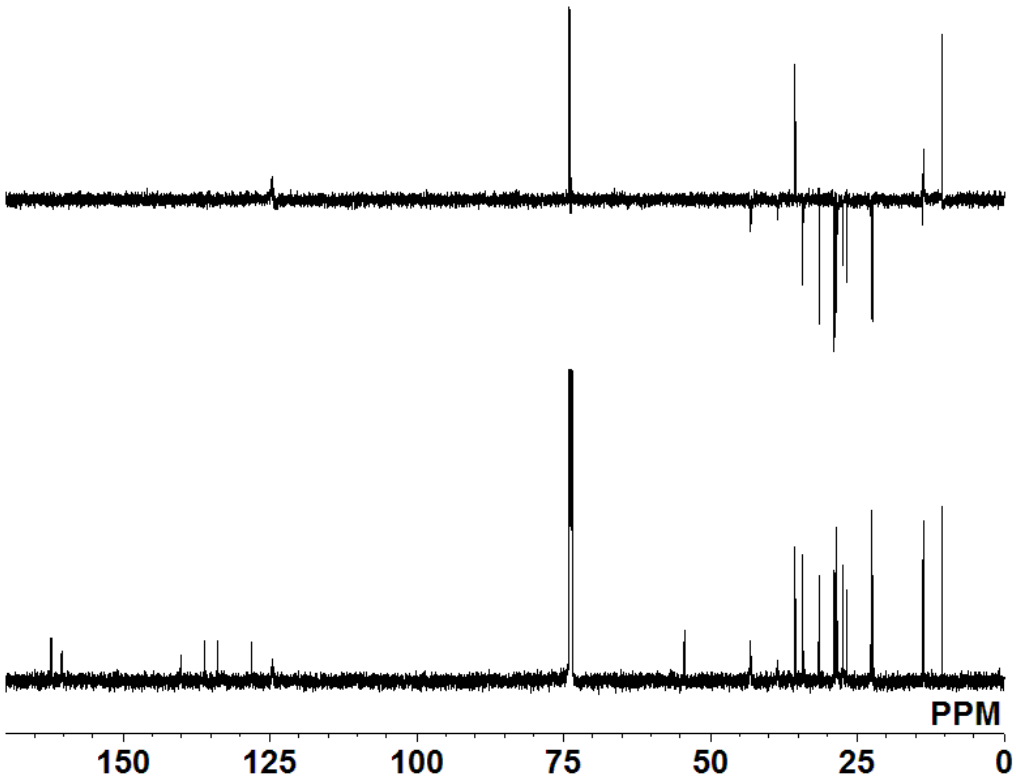

Figure S9. $^{13}C\{^{1}H\}$ and DEPT 135 NMR spectra of **P4** (150 MHz, $C_2D_2Cl_4$, 353 K).

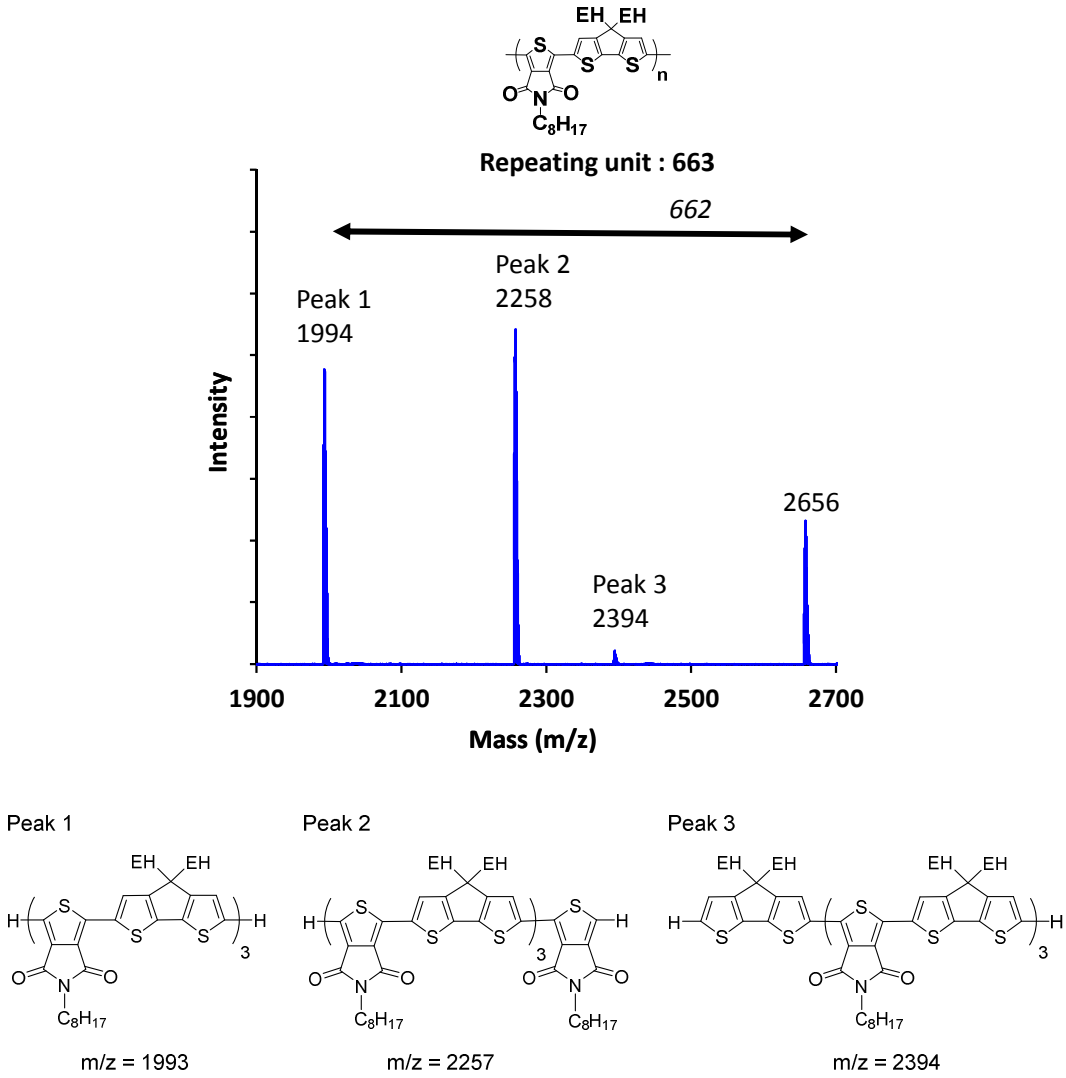

Figure S10. MALDI TOF MS spectrum of **P4**.

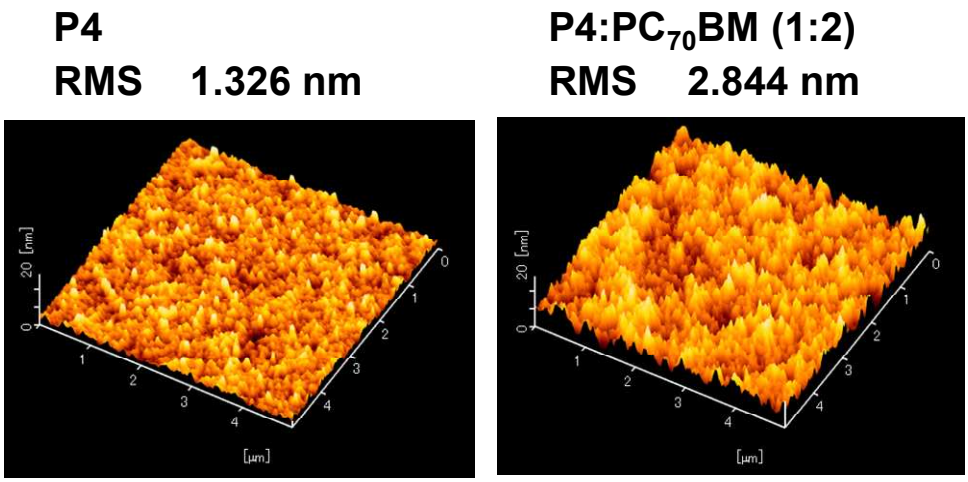

Figure S11. AFM images (5 × 5 μm^2) of **P4** and **P4**:$PC_{70}BM$ (1:2).

Table S1. Photovoltaic device characteristics of BHJ OPVs (Table 1, Entry 1)

	J_{sc} (mA/cm^2)	V_{oc} (V)	*FF*	PCE (%)
1	13.296	0.877	0.453	5.297
2	13.542	0.861	0.440	5.135
3	13.100	0.834	0.425	4.646
4	13.070	0.891	0.468	5.458
5	13.201	0.871	0.452	5.209
6	13.274	0.849	0.450	5.079
Average with standard deviation	13.3 ± 0.2	0.86 ± 0.02	0.45 ± 0.01	5.1 ± 0.3

ITO/ PEDOT:PSS/ **P4**:$PC_{70}BM$(1:2) (88 nm) / Al (80 nm)

The BHJ layer is fabricated using chlorobenzene + 1,8-diiodooctane 4% as solvent and annealed at 70 °C for 10 min.

Table S2. Photovoltaic device characteristics of BHJ OPVs (Table 1, Entry 2)

	J_{sc} (mA/cm^2)	V_{oc} (V)	*FF*	PCE (%)
1	13.294	0.917	0.536	6.547
2	13.940	0.913	0.535	6.815
3	13.825	0.885	0.530	6.493
4	13.107	0.903	0.523	6.196
5	13.148	0.897	0.517	6.112
6	13.088	0.890	0.523	6.098
Average with standard deviation	13.4 ± 0.4	0.90 ± 0.01	0.527 ± 0.008	6.4 ± 0.3

ITO/ PEDOT:PSS/ **P4**:$PC_{70}BM$(1:2) (90 nm) / LiF (1 nm)/ Al (80 nm)

The BHJ layer is fabricated using chlorobenzene + 1,8-diiodooctane 4% as solvent and annealed at 70 °C for 10 min.

Reference

S1. Chang, S. W.; Waters, H.; Kettle, J.; Kuo, Z. R.; Li, C. H.; Yu, C. Y.; Horie, M. *Macromol. Rapid Commun.* **2012**, *33* (22), 1927.